



1 Three-way Calibration Checks Using Ground-Based, Ship-Based 2 and Spaceborne Radars

3 Alain Protat ¹, Valentin Louf ¹, Joshua Soderholm ¹, Jordan Brook ², William Ponsoyby ³

4 ¹ Australian Bureau of Meteorology, Melbourne, Australia

5 ² University of Queensland, Brisbane, Australia

6 ³ Engineering and Technology Program, CSIRO National Collections and Marine Infrastructure, Hobart, Australia

7 *Correspondence to:* Alain Protat (alain.protat@bom.gov.au)

8 **Abstract.**

9 This study uses weather radar observations collected from *Research Vessel Investigator* to evaluate the Australian
10 weather radar network calibration monitoring technique that uses spaceborne radar observations from the NASA
11 Global Precipitation Mission (GPM). Quantitative operational applications such as rainfall and hail nowcasting
12 require a calibration accuracy of 1 dB for radars of the Australian network covering capital cities. Seven ground-
13 based radars along the coast and the ship-based OceanPOL radar are first calibrated independently using GPM radar
14 overpasses over a 3-month period. The calibration difference between the OceanPOL radar and each of the 7
15 operational radars is then estimated using collocated, gridded, radar observations to evaluate the accuracy of the
16 GPM technique. For all seven radars the calibration difference with the ship radar lies within ± 0.5 dB, therefore
17 fulfilling the 1 dB requirement. This result validates the concept of using the GPM spaceborne radar observations to
18 calibrate national weather radar networks (provided that the spaceborne radar maintains a high calibration accuracy).
19 The analysis of the day-to-day and hourly variability of calibration differences between the OceanPOL and Darwin
20 (Berrimah) radars also demonstrates that quantitative comparisons of gridded radar observations can accurately track
21 daily and hourly calibration differences between pairs of operational radars with overlapping coverage (daily and
22 hourly standard deviations of ~ 0.3 dB and ~ 1 dB, respectively).

23 **1 Introduction**

24 Operational radar networks play a major role in providing situational awareness and nowcasting in severe
25 weather situations, including heavy rain, flash floods, hailstorms, and wind gusts. Such radar-based information is
26 then used by forecasters as guidance for issuing severe weather warnings. The quality of these radar-derived
27 products in real-time is driven to a large extent by how well the underlying radar measurements are calibrated.
28 Recently, the Australian Bureau of Meteorology (BoM) has developed an operational radar calibration framework to
29 monitor the calibration and pointing accuracy of all BoM operational radars in real-time (Louf et al. 2019, hereafter
30 L19). As will be described in more detail later, this approach is based on a combination of three techniques,
31 allowing for an absolute calibration better than 1 dB, which is the operational calibration requirement in Australia
32 for quantitative use of the Australian weather radar observations over capital cities (so-called Tier 1 radars). At the
33 heart of this framework lies the so-called Volume Matching Method (VMM), initially developed by Schwaller and
34 Morris (2011) and further improved by Warren et al. (2018, hereafter W18). In this VMM technique, intersections



35 between individual ground-based radar beams and NASA Tropical Rainfall Measurement Mission (TRMM,
36 Simpson et al. 1996) or Global Precipitation Mission (GPM, Hou et al. 2014) scanning Ku-band radar beams are
37 averaged over an optimally defined common sampling volume (see W18 for more detail).

38 A major advantage of using the GPM VMM technique is that the spaceborne radar provides a single source
39 of reference to calibrate all radars of an operational network. Despite multiple possible sources of errors contributing
40 to the VMM calibration error estimate, such as temporal mismatch, imperfect attenuation corrections, gridding and
41 range effects, and differences in radar minimum detectable signal, the overall accuracy of such technique is thought
42 to be better than 2 dB for individual overpasses (Schwaller and Morris, 2011; W18; L19), but there has been no
43 independent quantification of this accuracy. This is the main objective of this study, where we use dual-polarization
44 C-band weather radar (OceanPOL) observations collected on board the Marine National Facility (MNF) Research
45 Vessel (RV) Investigator between Darwin and Perth, Australia, as part of the *Years of the Maritime Continent –*
46 *Australia* (YMCA, Protat et al. 2020) and the *Optimizing Radar Calibration and Attenuation corrections* (ORCA)
47 experiments to evaluate the approach of calibrating a whole radar network using GPM. The concept of this study is
48 presented in Fig. 1. The advantage of using a ship-based radar like OceanPOL relative to the GPM spaceborne radar
49 is that many of the error sources in ground-based / satellite radar comparisons are reduced to a minimum, allowing
50 for an upper bound for the natural variability of radar calibration to be estimated, as will be discussed later. In
51 section 2, we briefly describe the YMCA and ORCA experiments, the characteristics of radars used in this study,
52 and the calibration techniques. In section 3, we present the main findings of this study. Concluding remarks are
53 presented in section 4.

54 **2 Radar observations during YMCA and ORCA and calibration comparisons**

55 In this section, we briefly introduce the datasets collected during the YMCA and ORCA experiments, the
56 details of all radars involved in this study, and the techniques used to calibrate the ground and ship radars with the
57 spaceborne radar and to compare ground and ship radars.

58 **2.1 The YMCA and ORCA experiments**

59 *RV Investigator* OceanPOL radar observations used in this study were collected as part of two back-to-back
60 field experiments. The first experiment is the Australian contribution to the Years of the Maritime Continent
61 (YMCA), which is an international coordinated effort to better understand the organization of coastally induced
62 convection over the Maritime Continent and its complex interactions with large-scale drivers, with the ambition to
63 better represent these processes in global circulation models characterized by large and persistent rainfall biases.
64 During the second phase of YMCA (12 November – 19 December 2019), the sampling strategy was to position *RV*
65 *Investigator* off the coast around Darwin in a dual-Doppler configuration with either the Warruwi (north-east of
66 Darwin) or Berrimah (Darwin) operational C-band Doppler radars to characterize the rainfall, morphological, and
67 dynamical properties of convective systems developing near the coast and propagating offshore, which are
68 particularly poorly forecasted in this region (e.g., Neale and Slingo, 2002; Nguyen et al. 2017a,b), but are thought to
69 contribute about half of the rainfall along tropical coasts (e.g., Bergemann et al. 2015). In this study, we also take



70 advantage of the month-long time series of OceanPOL – Berrimah radar observations to quantify the variability of
71 radar calibration on daily and hourly timescales.

72 The second field experiment (ORCA) was conducted during a transit voyage to relocate *RV Investigator*
73 from Darwin to Perth, Western Australia. This transit voyage was an ideal opportunity to collect collocated radar
74 samples with several operational radars along the coast (Fig. 1). Specific stops of three hours were scheduled in the
75 vicinity of each radar in the event of precipitation within range of OceanPOL and of the ground-based radar. Of the
76 eight possible radars, we have luckily been able to collect such collocated precipitation samples for six of them,
77 except Geraldton and Carnarvon. In this study we will use all these collocated samples to quantify how well the
78 calibration estimate provided for each radar by the GPM technique agree with the calibration estimates obtained
79 using OceanPOL as a second and more accurate source of reference.

80 2.2 The radars involved in this study

81 Table 1 summarizes the relevant information about all radars used in this study. As clearly illustrated from
82 this table, the Australian radar network comprises a large variety of radars from different generations, frequencies
83 (although radars in this study are all C-band radars, but other parts of the country are covered by S-band radars),
84 beamwidths (ranging from 1.0° to 1.7°), range resolutions (ranging from 250m to 1000m), and total time to
85 complete the volumetric sampling (from 6 min for more recent radars to 10 minutes for older radars). At the time of
86 the YMCA and ORCA experiments, all radars operated continuously. The Berrimah (Darwin) and Serpentine
87 (Perth) radars are Tier 1 radars (as they cover capital cities), while all other radars in Table 1 are Tier 2 radars. Tier 1
88 and 2 radars have a calibration accuracy requirement of better than 1 and 2 dB, respectively.

89 The GPM KuPR and OceanPOL radars are the most modern radars. It must be noted that the OceanPOL
90 radar is the only dual-polarization radar. This important feature for several applications is not used in the present
91 study, except for the quality control of the OceanPOL radar data. Version 5 of the GPM 2AKu product has been
92 used for all comparisons in this study, which contains attenuation-corrected Ku-band reflectivities. GPM attenuation
93 correction is achieved using a hybrid approach combining the traditional Hitschfeld - Bordan technique (Hitschfeld
94 and Bordan, 1954) and the so-called Surface Reference Technique (Meneghini et al., 2004).

95 2.3 The dark art of radar calibration

96 Recently, BoM has developed the operational S³CAR (Satellite, Sun, Self-consistent, Clutter calibration
97 Approach for Radars) framework to monitor the calibration of the BoM operational radars in real-time (operational
98 version of L19). This approach is based on a combination of three techniques. The first technique, the Relative
99 Calibration Adjustment (RCA, e.g., L19; Wolff et al. 2015), assumes that the 95th percentile of "ground clutter"
100 radar reflectivities (buildings, topographic structures, trees, etc ...) within 10 km range is constant. This technique
101 tracks changes in daily calibration to better than 0.2 dB (L19) but does not provide an estimate of the absolute
102 calibration. The second technique (W18) statistically compares collocated ground radar and spaceborne Ku-band
103 radar from the NASA TRMM (1997-2014) and GPM (2014-present) missions, whose calibration is very accurately
104 tracked by NASA. From our experience, and as reported in L19, this technique provides an absolute calibration with
105 an accuracy of about 2 dB from each overpass. The S³CAR framework uses the RCA technique to detect stable
106 periods of calibration and averages calibration estimates from all GPM overpasses within each period, improving the



107 absolute calibration accuracy, hopefully to better than 1 dB. The third technique used in S³CAR is the solar
108 calibration technique, which is a faithful implementation of the Altube et al. (2015) method, with additional
109 corrections for a possible levelling error of the radars as described in Curtis et al. (2021). The solar calibration
110 technique uses sun power measurements collected at the Learmonth observatory, Western Australia. This technique
111 is mostly used in conjunction with the RCA and GPM outputs to diagnose whether a change of calibration is due to
112 the transmitting chain (RCA and GPM detect a change but not the solar calibration technique) or receiving chain (all
113 techniques detect a change). This is an important diagnostic to help radar engineers troubleshoot a radar issue and
114 enable rapid return to service.

115 Among all operational radars considered in this study, only two of these radars (Berrimah and Geraldton)
116 send the raw reflectivities to Head Office in real-time, allowing for the full S³CAR process to be used to calibrate
117 these radars. For the other radars, post-processing is done on-site to reduce the bandwidth required to send the radar
118 data in real-time (these radars are in very remote places). As a result, ground clutter and sun interference have been
119 removed for these radars, which implies that only the GPM part of the S³CAR framework can be used. As
120 explained, this reduces the accuracy of the calibration estimate for such radars.

121 **2.4 Statistical comparisons between OceanPOL and the ground radars**

122 Calibration between ground-based radars and OceanPOL proceeds by first gridding observations from each
123 radar to a common 1 km horizontal / 500 m vertical resolution domain, then building a joint frequency histogram of
124 reflectivity values from all common grid points. The expectation from such plots is that they should exhibit a
125 systematic shift, corresponding to a difference in calibration between the two radars, with a large amount of
126 variability in these comparisons owing to all the sources of errors involved in such comparisons (differences in exact
127 time of observations of a grid, imperfect attenuation corrections, gridding artefacts, differences in implicit resolution
128 of radar volumes at different ranges, differences in minimum detectable signal ...). The gridding technique used for
129 all radars is the same and follows Dahl et al. (2019). This gridding technique uses a constant radius of influence
130 (3.5km) and a weighted summation with distance to the centre of the grid for points belonging to the same elevation
131 angle but a linear interpolation between elevation angles in the vertical. This technique has the great advantage of
132 not producing the typical artificial vertical spreading of observations below / above the lowest / highest elevation
133 angles observed when using a radius of influence in all directions. Depending on how old the ground radars are,
134 different minimum reflectivity thresholds are used in the comparisons to mitigate potential artefacts in calibration
135 difference estimates due to the degraded sensitivity and reflectivity resolution of the older radars for low to
136 intermediate reflectivities. In general, a relatively high threshold of 20-25 dBZ was required, which also had the
137 advantage of reducing the potential impact of different non-uniform grid filling at the edges of the convective
138 systems due to different radar detection capabilities.

139 OceanPOL data have been corrected for attenuation using the Gu et al. (2011) C-band dual-polarization
140 technique available in the Py-ART toolkit (Helmus and Collis, 2016). The operational radars have been corrected for
141 attenuation using C-band reflectivity – attenuation relationships derived from the OceanRAIN dataset (Protat et al.
142 2019). It must be noted that additional comparisons done without attenuation corrections of the ground radars did
143 not yield large differences (less than 0.5 dB in all sensitivity tests conducted). This is presumably due to the fact that
144 there are many more points below 30-35 dBZ than above in those comparisons, resulting in a relatively minor
145 impact of attenuation on these statistical comparisons. Also, the ship and ground radars were generally not far away



146 from each other (typically 20-40 km), so the viewing geometry of the storms was quite similar from both radars in
147 most cases, resulting in similar levels of attenuation along the two different paths through the storms.

148 The scanning sequence employed for OceanPOL uses the exact same 14 elevation angles used throughout
149 the operational radar network. The start of each OceanPOL scanning sequence is synchronized with that of the
150 operational radars running a 6-minute sequence (starts on the hour then every 6 minutes), which implies that
151 temporal differences in volumes sampled by OceanPOL and the radars running the 6-minutes sequence are minimal.
152 The impact of temporal evolution on the comparisons between OceanPOL and the radars running a 10-minute
153 sequence will naturally be larger. To minimize this impact in our comparisons, we have discarded files for which the
154 start time differs from the OceanPOL start time by more than 2 min.

155 Finally, to mitigate the potential impact of wet radome attenuation at C-band on the comparisons, we have
156 screened out observations where precipitation was present within 5km of either of the radars from the comparisons.
157 More precisely, for each volumetric scan we estimate the precipitation fraction within 5 km, and if more than 20%
158 of this area is covered with precipitation, we conservatively discard this scan. However, it must be noted that results
159 obtained when changing that threshold were very similar, with maximum statistical differences in estimated
160 calibration difference less than 0.3 dB (not shown). From a visual inspection of radar scans, we inferred that this was
161 due to rainfall generally not observed over and around the radars when such comparisons were made.

162 **3 Results**

163 In this section, we present the main results of this three-way calibration comparison exercise. As illustrated
164 in Fig. 1, the first part of the calibration consistency check is to calibrate OceanPOL and the ground radars using the
165 same single independent source, the GPM spaceborne radar. All calibration results are summarized in Fig. 2. We are
166 fortunate enough that over two months including the YMCA and ORCA observational periods, the rainfall activity
167 allowed us to collect a reasonable number of GPM overpasses over each radar (except for Learmonth, radar 29, Fig.
168 2). As a result, for radar 29, we will use an older calibration estimate (-2.6 dB), derived from a GPM overpass with
169 many matched volumes in July 2019. Additional checks of the outputs of the RCA technique for radar 63 (discussed
170 later and shown as black dots in Fig. 4) indicated that the calibration of these two radars had not changed over that
171 period, which means that we can simply average all the estimates of calibration error from individual overpasses to
172 come up with a more accurate estimate for these radars. Looking at the time series of GPM calibration estimates for
173 other radars than 63 and considering the expected typical error of 2 dB for individual GPM overpasses as a
174 guideline, it seems reasonable to assume that the calibration of the OceanPOL, Waruwi (77), Dampier (15),
175 Broome (17), and Serpentine (70) radars has not changed over the observational period either, with fluctuations
176 around the mean calibration error estimate less than ~1.5 dB. The Port Hedland (16) radar is more problematic, as
177 the time series shows calibration error estimates ranging from -8 dB to -2.5 dB over that period. However, the three
178 overpass points closest to the date when collocated observations with OceanPOL were collected (26 December
179 2019) seem to agree reasonably well (around the mean value of -5 dB), so we will use this value of -5 dB in the
180 following but will keep in mind the lower confidence in this calibration figure.

181 The final step of this calibration consistency check study consists in using the OceanPOL radar (previously
182 calibrated using GPM, Fig. 2) as a second moving reference for the ground-based radars. In a perfect world, there



183 should be no statistical difference between OceanPOL and the ground-based radars since they have all been
184 calibrated using the same source of reference (GPM). However, as explained earlier, satellite – ground comparisons
185 are characterized by multiple sources of errors, including differences in sampled volumes (although great care is
186 taken to match sampling volumes as accurately as possible, e.g., Schwaller and Morris 2011, W18, L19), non-
187 uniform beam filling effects, temporal mismatch between observations, differences in minimum detectable signal,
188 and radar frequency differences requiring conversion (most problematic in the melting layer and ice phase of
189 convective storms where this correction is more uncertain, see W18). In comparison, ship radar – ground radar
190 comparisons, especially when radars are, as in this study, reasonably close to each other to minimize differences in
191 sampling volumes, are less prone to all these errors. The radar frequency is the same. The sampling volume and
192 temporal mismatches are also expected to be less problematic (but not entirely negligible, especially for the radars
193 running a 10-min sequence, see discussion in section 2.4). These more accurate ship – ground radar comparisons
194 should therefore be considered as an indirect evaluation of the GPM validation technique and if successful, a
195 demonstration of the value of using such GPM data as a single source of reference for the calibration of a whole
196 national network as is done in Australia with S³CAR.

197 Figure 3 shows a typical example of the 2D frequency histograms of reflectivity between OceanPOL and
198 the Berrimah radar (63) for one day (21 November 2019) of the YMCA experiment. Such frequency distribution
199 plots can be normalized in two different ways. If the number of points in each reflectivity pixel is divided by
200 the total number of points (as on the left panel of Fig. 3), it highlights where most of the comparison points are in the
201 reflectivity – reflectivity space, and therefore what contributes most to the mean calibration difference estimate.
202 When the number of points in each pixel is divided by the total number of points in each reflectivity bin on the x-
203 axis (right panel of Fig. 3), it provides a better visual sanity check of the systematic shift of the joint distribution
204 produced by the calibration difference over the whole reflectivity range and allows for other potential artefacts to be
205 detected. In the example of Fig. 3, which is typical of all comparisons made in this study, most of the points that
206 contributed to the estimation of the mean calibration difference of 0.9 dB between the two radars are clearly of
207 reflectivity less than 35 dBZ. On another hand, the right panel shows more clearly that there is indeed a consistent
208 shift in reflectivity values across the whole reflectivity range, as expected from a (systematic) calibration difference.
209 An important feature of Fig. 3 is the observed large variability around the mean calibration difference. The standard
210 deviation of calibration difference for all comparisons in this study and was typically between 4 and 6 dB. It must be
211 noted that this large standard deviation is an estimation of the errors on calibration difference of each individual
212 pixel, not that of the daily estimate. The higher number of days spent collecting collocated observations off the
213 Berrimah (63) and Waruwi (77) radars also offers an opportunity to estimate daily calibration differences and take a
214 closer look at the day-to-day variability of calibration differences. We will get back to that point shortly.

215 When including all days of observations for radars 63 and 77 (25 days for radar 63 and 4 days for radar 77
216 with precipitation), the mean calibration difference between OceanPOL and radars 63 and 77 are 0.4 dB and -0.3
217 dB, respectively (Fig. 4 for radar 63, Fig. 5a for radar 77, see also Table 2 for a summary of all calibration
218 differences found in this study). The next best operational radar is radar 70 (Perth). For this radar, only short
219 duration drizzle and scattered showers were observed when *RV Investigator* approached its destination (Fremantle
220 port), resulting in less points for the calibration difference estimate. Despite the short duration dataset for radar 70,
221 the 2D joint histogram of reflectivities show a consistent difference across the whole reflectivity range, with a mean



222 calibration difference of -0.4 dB (Fig. 5f). These three estimates are well below the required accuracy of 1 dB for
223 operational applications, which indicates that for these four good-quality radars (OceanPOL and radars 63, 77, and
224 70), the GPM comparisons provided a consistent calibration to within ± 0.5 dB. However, those are the comparisons
225 where errors were expected to be smallest, given the large number of days included in the comparisons for radars 63,
226 and the excellent synchronization of the 6-min scanning sequences with OceanPOL for these three radars.

227 Let us now turn our attention to the quantitative comparisons between OceanPOL and the older operational
228 radars (15, 16, 17, 29) running with a 10-minute scanning sequence and / or a degraded range resolution (as reported
229 in Table 1), and only a few opportunistic hours of collocated samples with precipitation (see list of time spans in
230 Table 2). Visual inspection of gridded radar data revealed the presence of strong anomalous propagation (AP) signal
231 in the lower levels (up to about 2km height ASL) for radars 15, 16, and 29, which has not been filtered correctly by
232 the operational radar post-processing suite. This problem is well known to the BoM forecasters. As a result, for these
233 radars, two sets of results are presented in Table 2. Calibration differences obtained from all data are labelled "AP"
234 and those obtained when screening out all common grids below 2km height are labelled "noAP". Figure 5 shows the
235 2D joint histograms of reflectivity when the anomalous propagation is screened out. The largest impact of
236 anomalous propagation is found for radar 16, with a difference of 0.9 dB between estimates with and without AP
237 screening. For the two other radars 15 and 29, the impact is modest (0.3 to 0.5 dB). This is due to the higher
238 proportion of samples located below 2 km height for the radar 16 case (not shown) than for the two other cases.
239 Overall, this result is shown to illustrate that particular attention needs to be paid in regions prone to anomalous
240 propagation effects. From Table 2 and Fig.5, the calibration differences with OceanPOL for these older radars are
241 +0.3 dB (radar 15), +0.1 dB (radar 16), +0.4 dB (Broome, radar 17), and +0.1 dB (radar 29). In summary, all seven
242 radars considered in these comparisons are characterized by calibration differences with OceanPOL within ± 0.5 dB,
243 despite the large variability in radar quality and number of samples included in the calibration difference estimates
244 (reported in Fig. 5). As a result, we can safely conclude that these comparisons validate the concept of using the
245 GPM VMM calibration technique as a single source of reference to accurately calibrate and monitor calibration of
246 national radar networks.

247 As introduced earlier, the day-to-day variability of calibration differences between ship and ground-based
248 radars can be analysed using the month of collocated samples between OceanPOL and the Berrimah radar collected
249 during YMCA (coloured points in Fig. 4). From Fig. 4, some simple statistics can be derived and discussed. The
250 minimum and maximum calibration differences over the month-long time series are -0.2 and +1.1 dB, which
251 corresponds to minimum and maximum differences of -0.6 and +0.7 dB around the mean value of 0.4 dB. The
252 colour of the points is the number of samples that were available to estimate the daily calibration difference. The
253 coloured error bars are estimates of the hourly standard deviation of calibration difference for each day, which will
254 be discussed in more detail later. From a close inspection of the location of points with respect to the mean value for
255 the period, there does not seem to be any obvious relationship between the number of points and how close the
256 estimates are to the mean value of 0.4 dB. This result shows that the number of samples is not the main source of
257 differences between daily estimates.

258 The standard deviation of daily calibration difference between Berrimah and OceanPOL over this month of
259 data is 0.33 dB (Fig. 4). Since this standard deviation value includes any potential natural variability of the daily
260 calibration difference and the variability due to uncertainties in these daily ship – ground radar comparisons such as



261 spatial resolution differences and temporal mismatches, this value of 0.33 dB can be considered as an upper bound
262 for the uncertainty in daily calibration difference estimates. To check whether the natural variability of daily radar
263 calibration was minimal over that month of Darwin observations, we have added in Fig. 4 the time series of daily
264 mean RCA values (black points) used as part of our operational S³CAR calibration monitoring technique as another
265 calibration variability metrics. It has been shown that this RCA technique could track changes in daily calibration to
266 better than about 0.2 dB (L19). To better compare variabilities obtained from calibration differences and the RCA,
267 we have subtracted the mean RCA (54.11 dBZ) value to each daily RCA value and added the mean calibration
268 difference over the whole period (0.4 dB), so that the daily RCA time series is centred on the mean calibration
269 difference (blue line). Over this whole period, the standard deviation of the RCA value is 0.12 dB, which confirms
270 the L19 results. This standard deviation is smaller than that of the OceanPOL – Berrimah comparisons (0.33 dB). If
271 we assume that the standard deviation of the RCA value is an upper bound for the natural variability of the daily
272 calibration figure, this result shows that most of the variability in calibration difference between the OceanPOL and
273 Berrimah radars (0.33 dB) is in fact a measure of the inherent uncertainties of gridded radar comparisons. This
274 important result highlights that such quantitative comparisons of overlapping gridded radar observations can be
275 successfully used to monitor the consistency of daily calibration of operational radars with overlapping coverage to
276 better than the 1 dB requirement.

277 The last thing we explore with this Darwin dataset is the potential for tracking calibration differences at the
278 hourly time scale rather than the daily time scale. To do so, for each day of observations, we have estimated the
279 calibration difference from 1-hour chunks of collocated data, then estimated the standard deviation of the hourly
280 estimates for each day. An example of such daily analysis is shown in Fig. 6 for a day (08/12/2019) where 15
281 successive hours of collocated samples were available. Although this example includes more hours of comparisons
282 than most other days, it is very typical in terms of the hour-to-hour variability we observe each day, making it a
283 good candidate for illustrative purposes. We have not elected to screen out hours with fewer points, which, as can be
284 seen from hours 14 and 15, would have resulted in a lower hourly standard deviation for that case. This should
285 probably be done in an operational implementation. In this respect, the standard deviation of hourly calibration
286 difference presented in Fig. 4 can be considered as an upper bound for the hourly standard deviation. The hourly
287 standard deviation is shown in Fig.6 as a red error bar on top of the daily average point, and as a coloured error bar
288 over each daily average in Fig. 4. Over the 1-month study period, the average hourly standard deviation derived
289 from all daily estimates is 0.8 dB, which is within the 1 dB requirement, but the two extreme values are 0.5 and 1.5
290 dB (Fig. 4), indicating that occasionally the hourly estimates of calibration difference would not fully meet this
291 requirement. From Fig. 4, it also appears that there is no inverse relationship between the number of samples and the
292 hourly standard deviation, which could have perhaps been expected. For instance, the two points with highest hourly
293 standard deviation (02 and 06 December 2019) are at both ends of the number of samples spectrum, and the three
294 points with the lowest hourly standard deviations are in the lower half of the number of samples spectrum. Fig.4 also
295 shows that when using the hourly standard deviation as an error bar, the mean value over that period (0.4 dB) is
296 always included within one standard deviation of the daily estimate. These results would obviously need to be
297 confirmed with more observations in the future but do highlight the potential for hourly tracking of calibration
298 differences, enabling very early detection of issues with operational radars.

299



300 4 Conclusions

301 In this study, we have used collocated observations between spaceborne, ship-based, and ground-based
302 radars collected during the YMCA (off Darwin) and ORCA (transit voyage between Darwin and Perth) experiments
303 to gain further insights into the suitability and accuracy of using spaceborne radar observations from the GPM
304 satellite mission to calibrate national operational radar networks. A major advantage of using a single source of
305 reference is that all radars of the network are calibrated in the same way. Error estimates in the literature (Schwaller
306 and Morris, 2011; W18; L19) hint at a value of about 2 dB from individual GPM overpasses to better than 1 dB
307 when stable periods of calibration can be estimated using the RCA technique and individual GPM estimates can be
308 averaged.

309 Using collocated weather radar observations between the OceanPOL radar on *RV Investigator* and 7
310 operational radars off the northern and western coasts of Australia (all calibrated using GPM), we found that for all
311 seven operational radars, the calibration difference with OceanPOL was within ± 0.5 dB, well within the 1 dB
312 requirement for quantitative radar applications (-0.3, +0.4, +0.4, +0.1, +0.3, +0.1, and -0.4 dB). This important result
313 validates the concept of using the GPM spaceborne radar observations to calibrate national weather radar networks.

314 From the longer YMCA dataset collected when *RV Investigator* was stationed off the coast of Darwin for
315 about a month, the day-to-day variability of calibration differences between the OceanPOL and Darwin (Berrimah)
316 radars was estimated and compared with the daily calibration variability estimated using the RCA technique. From
317 these comparisons, we have found that the natural variability of daily radar calibration was small over our month of
318 observations (~ 0.1 dB daily standard deviation). These comparisons also demonstrated that the intercomparison of
319 gridded radar observations had the potential to estimate calibration differences between radars with overlapping
320 coverage to within about 0.3 dB at daily time scale and about 1 dB at hourly time scale. Such technique will be
321 added to our operational S³CAR calibration monitoring framework as an additional calibration monitoring reference
322 between GPM overpasses when the RCA technique cannot be applied.

323 Acknowledgments

324 The Authors wish to thank the CSIRO Marine National Facility (MNF) for its support in the form of *RV Investigator*
325 sea time allocation on Research Voyages IN2019_V06 (YMCA) and IN2019_T03 (ORCA), support personnel,
326 scientific equipment, and data management. Tom Kane and Mark Curtis from BoM are also warmly thanked for
327 always patiently answering our relentless questions about the Australian weather radar network intricacies.

329 Code availability

330 Codes developed for this study are protected intellectual property of the Bureau of Meteorology and are not publicly
331 available.

333 Data availability

334 All OceanPOL and Level 1b data from the operational radar network used in this study are available at
335 <http://www.openradar.io>. The NASA GPM radar data were obtained using the STORM online data access interface
336 to NASA's precipitation processing system archive (<https://storm.pps.eosdis.nasa.gov>).

337



338 **Sample availability**

339 No samples were used in this study.

340

341 **Author contribution**

342 AP, JS, VL, JB, and WP collected the datasets used in this study. VL produced the GPM comparisons using the
343 operational S3CAR technique. JS produced post-processed volumetric and gridded data for all ground-based radars.
344 VL produced the gridded OceanPOL data. JB developed the gridding technique used in this study. AP designed and
345 coordinated the YMCA and ORCA field experiments, analyzed the results, and wrote the manuscript. VL, JS, JB,
346 and WP provided edits of the manuscript.

347

348 **Competing interests:**

349 The authors declare that they have no conflict of interest.

350 **References**

- 351 Altube, P., J. Bech, O. Argemi, and T. Rigo: Quality control of antenna alignment and receiver calibration using the
352 sun: Adaptation to midrange weather radar observations at low elevation angles. *J. Atmos. and Ocean. Technol.*,
353 32, 927-942, <https://doi.org/10.1175/JTECH-D-14-00116.1>, 2015.
- 354 Bergemann, M. M., C. Jakob, and T. P. Lane: Global detection and analysis of coastline-associated rainfall using an
355 objective pattern recognition technique. *Journal of Climate*. 28, 18, p. 7225-7236, 2015.
- 356 Curtis, M., G. Dance, V. Louf, and A. Protat: Diagnosis of Tilted Weather Radars Using Solar Interference. *J.*
357 *Atmos. Oceanic Tech.*, in Press, June 2021.
- 358 Dahl, N. A., A. Shapiro, C. K. Potvin, A. Theisen, J. G. Gebauer, A. D. Schenkman, and M. Xue: High-Resolution,
359 Rapid-Scan Dual-Doppler Retrievals of Vertical Velocity in a Simulated Supercell. *J. Atmos. and Ocean.*
360 *Technol.*, 36, 1477-1500, DOI: 10.1175/JTECH-D-18-0211.1, 2019
- 361 Gu, J.-Y., A. Ryzhkov, P. Zhang, P. Neilley, M. Knight, B. Wolf, and D.-I. Lee: Polarimetric Attenuation
362 Correction in Heavy Rain at C Band. *Journal of Applied Meteorology and Climatology*, 50(1), 39–58.
363 <https://doi.org/10.1175/2010JAMC2258.1>, 2011.
- 364 Helmus, J. J., and S. M. Collis.: The Python ARM Radar Toolkit (Py-ART), a Library for Working with Weather
365 Radar Data in the Python Programming Language. *Journal of Open Research Software*, 4(1), e25.
366 <https://doi.org/10.5334/jors.119>, 2016.
- 367 Hitschfeld, W., and J. Bordan: Errors inherent in the radar measurement of rainfall at attenuating wavelengths.
368 *J.Meteor.*, 11, 58–67, [https://doi.org/10.1175/1520-0469\(1954\)011.0058](https://doi.org/10.1175/1520-0469(1954)011.0058): EIITRM.2.0.CO;2, 1954.
- 369 Hou, A. Y., and Coauthors: The Global Precipitation Measurement mission. *Bull. Amer. Meteor. Soc.*, 95, 701–722,
370 <https://doi.org/10.1175/BAMS-D-13-00164.1>, 2014.
- 371 Louf, V., A. Protat, C. Jakob, R. A. Warren, S. Rauniyar, W. A. Petersen, D. B. Wolff, and S. Collis: An integrated
372 approach to weather radar calibration and monitoring using ground clutter and satellite comparisons. *J. Atmos.*
373 *Oceanic Tech.*, 36, 17-39, 2019. (L19)
- 374 Meneghini, R., J. Jones, T. Iguchi, K. Okamoto, and J. Kwiatkowski: A hybrid surface reference technique and its
375 application to the TRMM precipitation radar. *J. Atmos. Oceanic Technol.*, 21, 1645–1658,
376 <https://doi.org/10.1175/JTECH1664.1>, 2004.



377 Neale, R., and J. Slingo: The maritime continent and its role in the global climate: A GCM study, *J. Clim.*, 16, 834–
 378 848, 2002.

379 Nguyen, H., C. Franklin, and A. Protat: Understanding model errors over the Maritime Continent using CloudSat
 380 and CALIPSO simulators. *Quart. J. Roy. Meteor. Soc.*, DOI:10.1002/qj.3168, 2017.

381 Nguyen, H., A. Protat, L. Rikus, H. Zhu and M. Whimpey: Sensitivity of the ACCESS forecast model statistical
 382 rainfall properties to resolution. *Quart. J. Roy. Meteor. Soc.*, DOI:10.1002/qj.3056, 2017.

383 Protat, A. and I. McRobert: Three-dimensional wind profiles using a stabilized shipborne cloud radar in wind
 384 profiler mode. *Atmos. Meas. Tech.*, 13, 3609–3620, <https://doi.org/10.5194/amt-13-3609-2020>, 2020.

385 Protat, A., C. Klepp, V. Louf, W. Petersen, S. P. Alexander, A. Barros, and G. G. Mace: The latitudinal variability
 386 of oceanic rainfall properties and its implication for satellite retrievals. Part 2: The Relationships between Radar
 387 Observables and Drop Size Distribution Parameters. *J. Geophys. Res. Atmos.*, 124, 13312-13324,
 388 <https://doi.org/10.1029/2019JD031011>, 2019.

389 Schwaller, M. R., and K. R. Morris: A ground validation network for the Global Precipitation Measurement mission.
 390 *J. Atmos. Oceanic Technol.*, 28, 301–319, <https://doi.org/10.1175/2010JTECHA1403.1>, 2011.

391 Simpson, J., C. Kummerow, W.-K. Tao, and R. F. Adler: On the Tropical Rainfall Measuring Mission (TRMM).
 392 *Meteor. Atmos. Phys.*, 60, 19–36, <https://doi.org/10.1007/BF01029783>, 1996.

393 Warren, R. A., A. Protat, V. Louf, S. T. Siems, M. J. Manton, H. A. Ramsay, and T. Kane: Calibrating ground-based
 394 radars against TRMM and GPM. *J. Atmos. Oceanic Technol.*, 35, 323-346, 2018. (W18)

395 Wolff, D. B., D. A. Marks, and W. A. Petersen: General application of the relative calibration adjustment (RCA)
 396 technique for monitoring and correcting radar reflectivity calibration. *J. Atmos. Oceanic Technol.*, 32, 496–506,
 397 <https://doi.org/10.1175/JTECH-D-13-00185.1>, 2015.

398

399 **Tables**

Radar ID or Platform	Name	Make	(lat, lon)	Band	ω (°)	Δr (m) / Δt (min)
GPM	KuPR	N/A	Variable	Ku	0.7	125 / NA
RV Investigator	OceanPOL	DWSR-2501C-SDP	Variable	C	1.3	125 / 6
15	Dampier	WSR81C	(-20.654; 116.683)	C	1.7	1000 / 10
16	Port Hedland	TVDR2500-8	(-20.372; 118.632)	C	1.7	500 / 10



17	Broome	DWSR2502C-8	(-17.948; 122.235)	C	1.7	500 / 10
29	Learmonth	TVDR2500-8 (Digital upgrade)	(-22.103; 113.999)	C	1.7	250 / 10
63	Berrimah (Darwin)	DWSR2502C-14	(-12.456; 130.927)	C	1.0	250 / 6
70	Serpentine (Perth)	TVDR2500-14	(-32.392; 115.867)	C	1.0	500 / 6
77	Waruwi	DWSR2502C-14	(-11.648; 133.380)	C	1.0	250 / 6

400 Table 1: Main characteristics of the radars used in this study: radar ID in the operational radar network or platform,
 401 name, make, coordinates, frequency band, beamwidth ω ($^\circ$), range bin size Δr (m), and total time to complete the
 402 volumetric sampling Δt (min). OceanPOL and all ground-based radars have been manufactured by the Enterprise
 403 Electronics Corporation (EEC).

Date	Time Span (UTC)	Radar	Calibration Error (Radar – OceanPOL)
20191115	04:00 – 07:00	77	-0.2
20191117	04:00 – 08:00	77	+0.5
20191127	06:00 – 11:00	77	-0.2
20191128	03:00 – 07:00	77	-0.6
All dates above	All time spans above	77	-0.3
All dates in Fig. 4	Miscellaneous	63	+0.4
20191225	12:00 – 21:00	17	+0.4
20191226	18:00 – 24:00	16	-0.8 (AP) / +0.1 (noAP)
20191227	08:00 – 11:00	15	-0.2 (AP) / +0.3 (noAP)



20191228	08:00 – 11:00	29	-0.2 (AP) / +0.1 (noAP)
20200102	03:00 – 05:00	70	-0.4

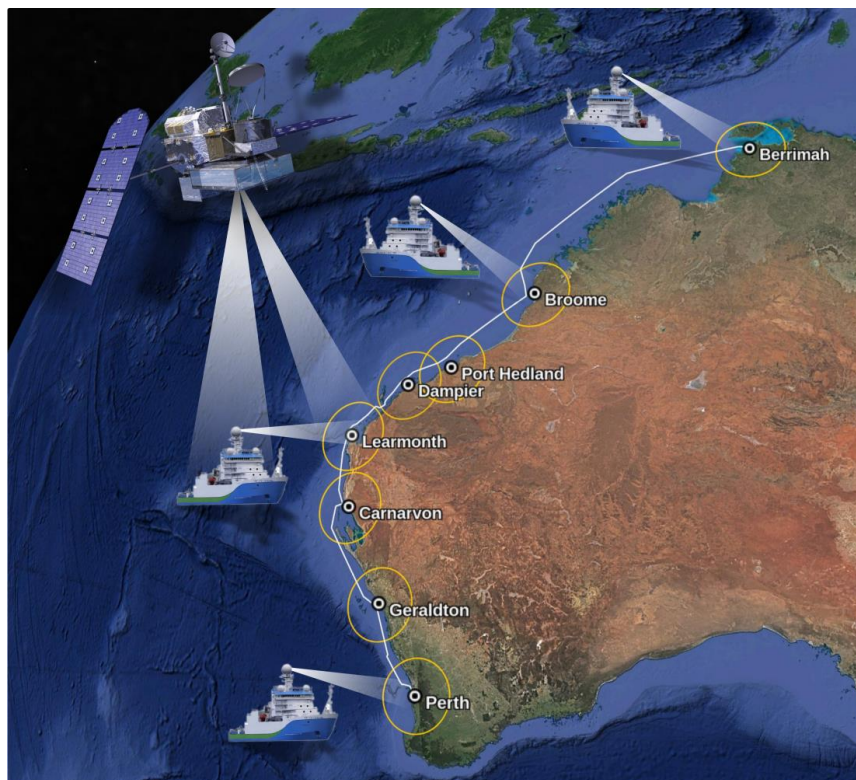
404 Table 2: Ground radar – OceanPOL calibration difference estimates for all comparisons of this study. A mean
405 calibration difference for radars 63 and 77 that includes all dates and time spans is also provided. For radars 15, 16,
406 and 29, two estimates are provided, with no test on minimum height (AP) or with a minimum height of 2 km for the
407 comparisons (noAP), in an attempt to remove residual anomalous propagation artefacts observed for these radars.

408

409

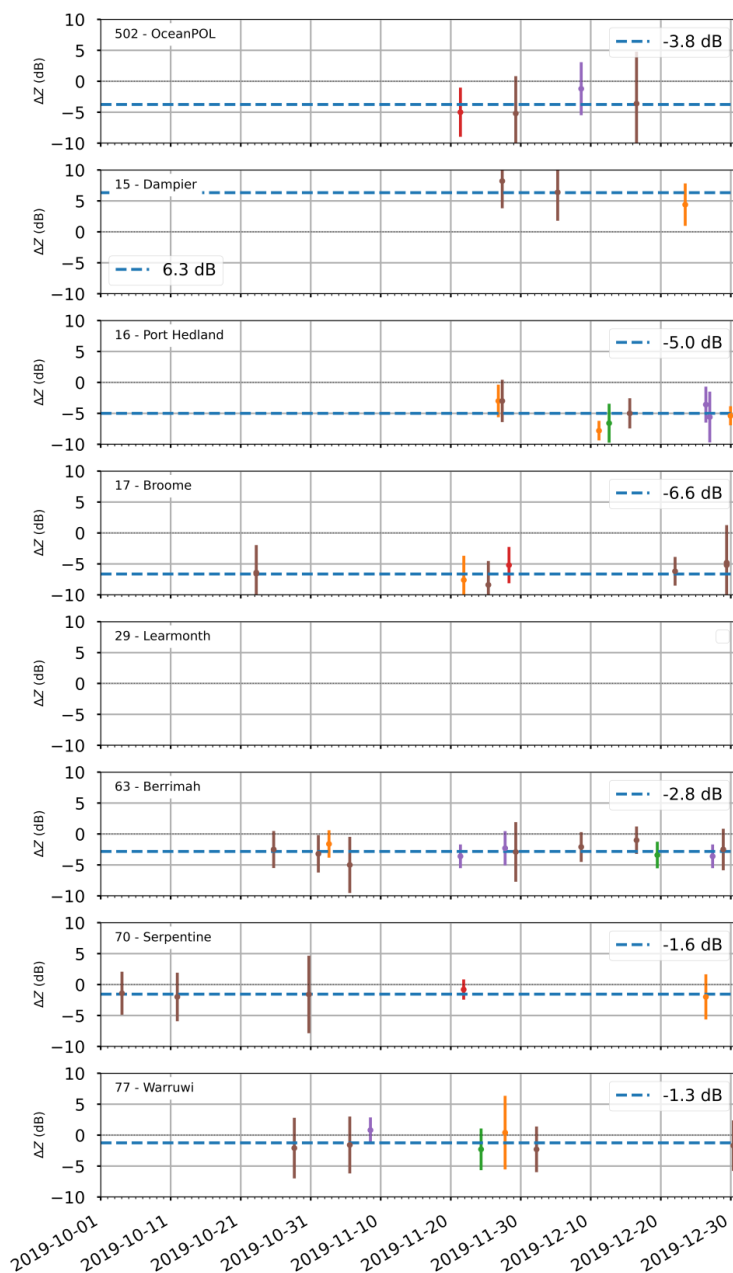


410 **Figures**



411

412 **Figure 1: The concept of this study. Ship-based OceanPOL radar and ground-based radars are calibrated independently**
413 **using the GPM Ku-band spaceborne radar, then all ground radars are compared with OceanPOL during the ORCA**
414 **voyage as RV Investigator sails south. The 150 km radius of each radar is shown by a yellow circle and the ship track is**
415 **shown using a white line. © 2021 Google Earth; Map Data: SIO, NOAA, U.S. Navy, NGA, GEBCO; Map Image:**
416 **Landsat/Copernicus.**

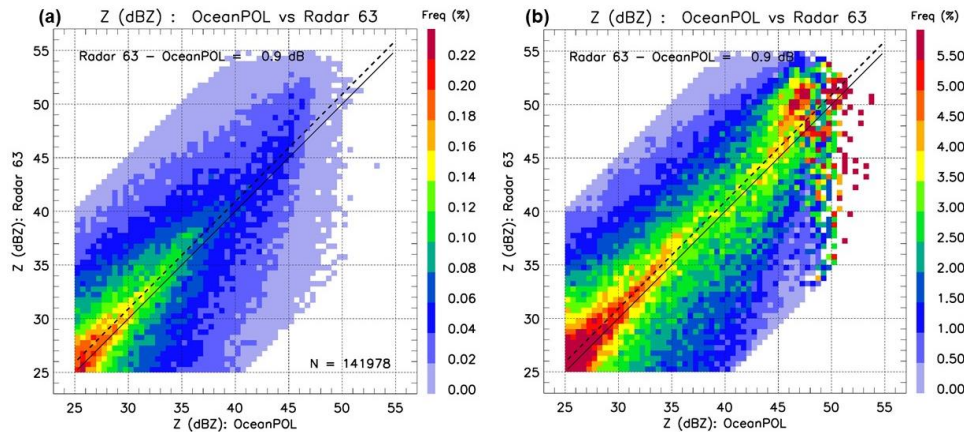


417

418 **Figure 2: Individual calibration error estimates from the GPM comparisons, for all radars used in this study. The**
 419 **standard deviation of the PDF of reflectivity difference is also shown for each estimate as an error bar. The mean value**
 420 **over the whole period is displayed as a dashed line for each radar, and the value is reported on the upper-right of each**
 421 **panel. Note that a negative value mean that the radar is under-calibrated (radar – GPM). The colour of each overpass**
 422 **point is the number of matched volumes: less than 20 (blue), 20 to 60 (orange), 60 to 100 (green), 100 to 150 (red), 150 to**
 423 **200 (purple) or more than 250 (brown).**



424

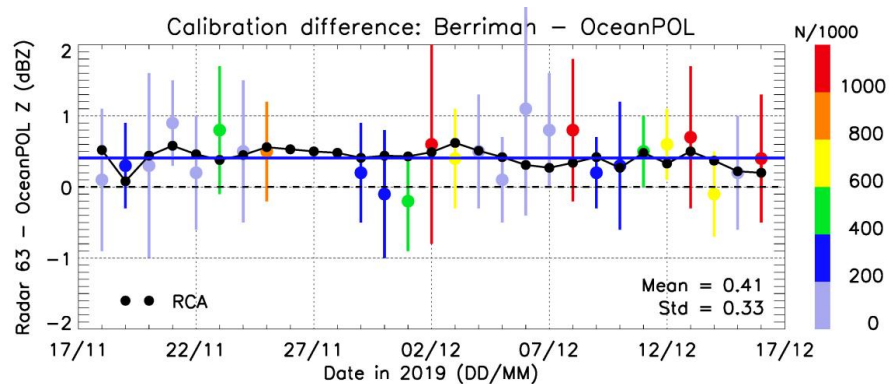


425

426 **Figure 3:** Illustration of 2D joint frequency histograms of reflectivity used to compare quantitatively the OceanPOL radar
 427 (x-axis) and any of the ground-based radar (y-axis). For each plot, the 1:1 line is drawn as a solid line, and the calibration
 428 difference estimate is written and shown as a dashed line. The colours show the frequency of points falling in each pixel of
 429 the 2D joint histograms, either expressed as the % of the total number of points (panel a) or as a % of the sum of points
 430 for each value of OceanPOL reflectivity (i.e., sum of all points along the y-axis at each constant value of the x-axis). The
 431 pixel size used for these plots is 0.5 dB. The number of samples N is also written in panel a.

432

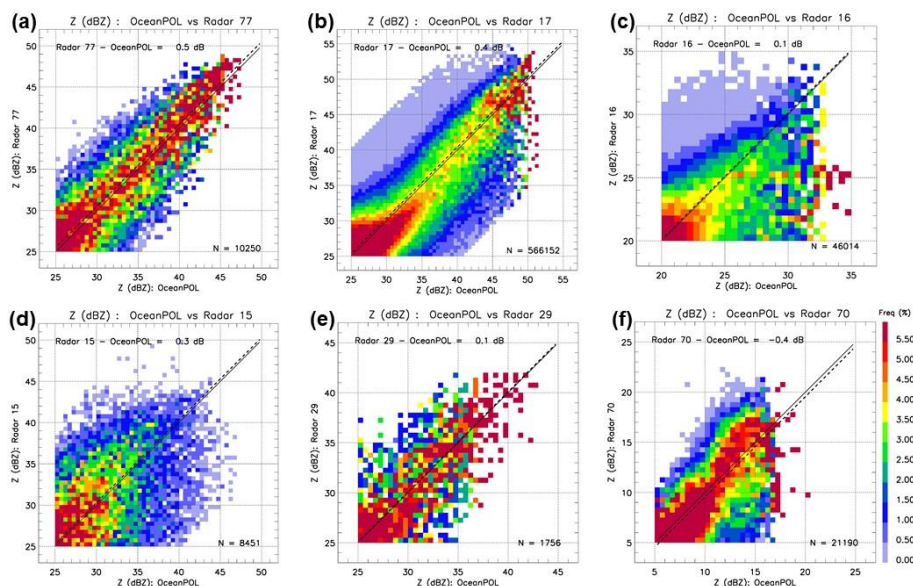
433



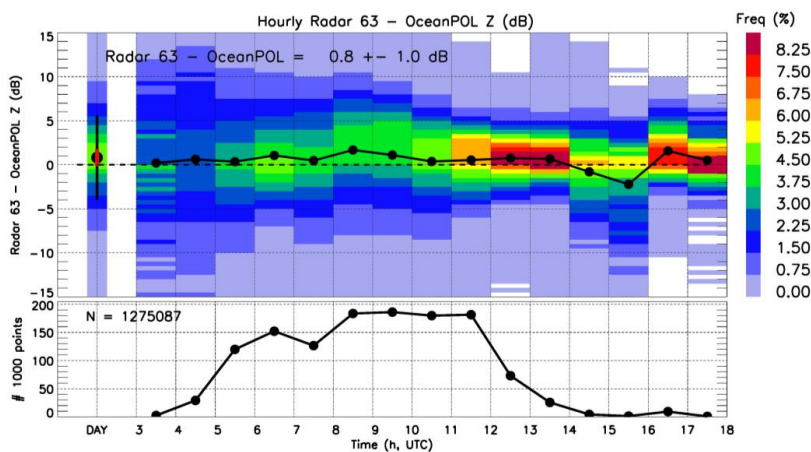
434

435

436 **Figure 4:** Time series of calibration differences between OceanPOL and radar 63 (Berrimah) during the YMCA
 437 experiment. Each coloured point is a daily estimate of calibration difference. The colour of the point is the number of
 438 points for each comparison, and the coloured error bar is the standard deviation of hourly calibration difference
 439 estimates for that day (see text and Fig. 6 for more details). The solid blue line is the mean value obtained from all these
 440 daily estimates (0.4 dB). The overall mean and standard deviation of the daily calibration difference over the period of
 441 observations are also written on the lower-right side of the figure. The black dashed line is the zero line. The black points
 442 are the daily outputs of the RCA values, with the mean RCA value over the period subtracted and the mean value of
 443 calibration difference added, so that the time series is centred on the mean calibration difference value.



444
 445 **Figure 5:** 2D joint histograms of reflectivity as in Figure 3b but for radars (a) 77, (b) 17, (c) 16, (d) 15, (e) 29, and (f) 70.
 446 Values of calibration differences are also reported in Table 2. The number of samples N is also given in each panel.
 447



448
 449 **Figure 6:** Hourly analysis of calibration differences between Berrimah (radar 63) and OceanPOL for a selected day
 450 (08/12/2019). The upper panel shows each hourly calibration estimate as a black dot, as well as the full frequency
 451 distribution of differences within each hour (colours). The first column of the upper-panel shows the daily summary,
 452 including the mean value (black dot, value is also written), the frequency distribution of calibration differences (colours),
 453 the standard deviation of the difference using the N collocated samples (black error bar), and the standard deviation of
 454 the hourly estimates of calibration differences for that day (red error bar, value is also written). Lower panel shows the
 455 number of samples in each hour (note y axis is the number of points divided by 1000) and the total number of samples N
 456 is also provided.